ENERGY
CONVERSION &
MANAGEMENT

Nonlinear modeling and identification of a DC motor for bidirectional operation with real time experiments

Tolgay Kara *, İlyas Eker

*Department of Electrical and Electronics Engineering, Division of Control Systems,
University of Gaziantep, 27310 Gaziantep, Turkey*

Abstract

Modeling and identification of mechanical systems constitute an essential stage in practical control design and applications. Controllers commanding systems that operate at varying conditions or require high precision operation raise the need for a nonlinear approach in modeling and identification. Most mechanical systems used in industry are composed of masses moving under the action of position and velocity dependent forces. These forces exhibit nonlinear behavior in certain regions of operation. For a multi-mass rotational system, the nonlinearities, like Coulomb friction and dead zone, significantly influence the system operation when the rotation changes direction. The paper presents nonlinear modeling and identification of a DC motor rotating in two directions together with real time experiments. Linear and nonlinear models for the system are obtained for identification purposes, and the major nonlinearities in the system, such as Coulomb friction and dead zone, are investigated and integrated in the nonlinear model. The Hammerstein nonlinear system approach is used for identification of the nonlinear system model. Online identification of the linear and nonlinear system models is performed using the recursive least squares method. Results of the real time experiments are graphically and numerically presented, and the advantages of the nonlinear identification approach are revealed.
© 2003 Elsevier Ltd. All rights reserved.

Keywords: Nonlinear modeling; Nonlinear identification; Hammerstein system; DC motor; Coulomb friction; Dead zone

---

* Corresponding author. Tel.: +90-342-360-1200x2132; fax: +90-342-360-1103.
E-mail address: kara@gantep.edu.tr (T. Kara).

1. Introduction

A sound knowledge of the system characteristics is of primary importance in any industrial application [1]. For process control and automation purposes, a detailed analysis of the plant with its every component should be performed. Especially, control selection and design for high performance electromechanical systems requires the availability of detailed information about the components of the plant, with its linear and nonlinear, static and dynamic characteristics [1,2]. For such systems, the assumption that the nonlinearities are negligible leads to loss in the generality of the results obtained [1]. DC motors, as components of electromechanical systems, are widely used as actuating elements in industrial applications for their advantages of easy speed and position control and wide adjustability range [3]. Consequently, examination of DC motor behavior constitutes a useful effort for analysis and control of many practical applications [1–3]. In modeling a DC motor connected to a load via a shaft, the general approach is to neglect the nonlinear effects and build a linear transfer function representation for the input–output relationship of the DC motor and the load it drives [1,4]. This assumption is satisfactorily accurate and valid as far as conventional control problems are concerned. However, when the DC motor operates at low speeds and rotates in two directions, or when it has a wide range of operation and high precision control is needed for the application, the assumption that the nonlinear effects on the system are negligible may lead to intolerably high modeling errors and result in poor control performance [1,3].

When the physical system structure and parameters are unavailable or dependent on time or operating conditions, a mathematical model representing the system behavior may not be obtainable. For this case, the system parameters should be obtained using a system identification procedure [5,6]. Identification of linear systems is a rather old field of study, and many methods are available in the literature [5,6]. However, identification of nonlinear systems is a relatively new topic of interest [5–7]. In mechanical systems with a DC motor, identification is an occasionally employed procedure for examination and detection of the system parameters. The nonlinear identification of DC motors has also been of interest in recent years, together with compensation for nonlinearities like Coulomb friction, backlash and stick-slip effect [8–10]. This paper basically focuses on nonlinear modeling and identification of a mechanical system with a DC motor rotating in two directions with Coulomb friction and dead zone nonlinearities. The nonlinear system model is built and a nonlinear Hammerstein structure is used for the identification procedure.

2. Model of system dynamics

Accurate model building is a crucial stage in practical control problems. An adequately developed system model is essential for reliability of the designed control. When the plant has uncertainties or time dependencies, or cannot be parameterized, a model for the system may be hard to obtain. For such systems, the system parameters should be determined using system identification techniques. However, an appropriate model structure should be obtained before the identification procedure can be executed [6]. Consequently, the system modeling process is vital for control and identification problems. In modeling the DC motor, the aim is to find the governing differential equations that express the motor characteristics and relate the applied voltage to

the torque produced by the rotor [11]. A schematic diagram of the DC motor built with regard to the aim expressed above is given in Fig. 1. The diagram shows the electrical components of the overall rotational system [3]. The equations that describe the motor electrical components are as follows [9]:

$$v_a = R_a i_a + L_a \left(\frac{di_a}{dt} \right) + e_a \tag{1}$$

$$e_a = K_m \omega_m \tag{2}$$

$$T_m = K_m i_a \tag{3}$$

where v_a (V) is the motor armature voltage, R_a (Ω) is the armature coil resistance, L_a (H) is the armature coil inductance, i_a (A) is the armature current, e_a (V) is the back electromotive force, K_m (Vs/rad) is the motor's torque constant, T_m (Nm) is the torque developed by the motor and ω_m (rad/s) is the rotational speed of the motor.

Like most rotational systems, the system in consideration can be modeled as a multi-mass system with the masses connected with flexible shafts or springs [9]. The model can be simplified further as a two mass system connected by a mass or inertia free flexible shaft, where the first mass represents the DC motor, and the second mass represents the total load that the motor rotates. A schematic diagram of the simplified two mass system is illustrated in Fig. 2.

In modeling the dynamics of the simplified two mass system, considering only the linear dynamics or approximating the model as a linearized one is a common approach [4,9]. However, the validity of the linear approximation and the sufficiency of the linearized dynamics in recovering the system nonlinearities depend on the operating point and speed span of the rotational system [12,13].

For the case that the system can be accurately modeled without considering the major nonlinear effects by the speed dependent friction, dead time and time delay, a linear model for the two
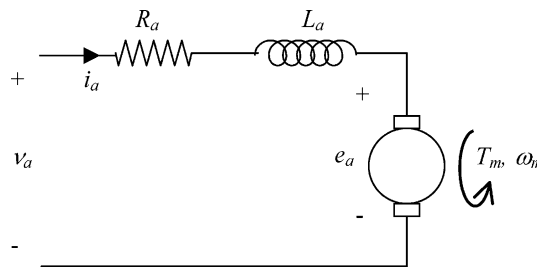

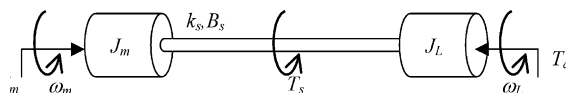Fig. 1. A schematic diagram of the permanent magnet DC motor.

Fig. 2. A schematic diagram of the two mass rotational system.

mass mechanical system schematically given in Fig. 2 can be obtained using the conventional torque balance rule [9]:

$$J_{\mathrm{m}}\left(\frac{\mathrm{d}\omega_{\mathrm{m}}}{\mathrm{d}t}\right) = T_{\mathrm{m}} - T_{\mathrm{s}} - B_{\mathrm{m}}\omega_{\mathrm{m}} \tag{4}$$

$$J_{\mathrm{L}}\left(\frac{\mathrm{d}\omega_{\mathrm{L}}}{\mathrm{d}t}\right) = T_{\mathrm{s}} - B_{\mathrm{L}}\omega_{\mathrm{L}} - T_{\mathrm{d}} \tag{5}$$

$$T_{\mathrm{s}} = k_{\mathrm{s}}(\theta_{\mathrm{m}} - \theta_{\mathrm{L}}) + B_{\mathrm{s}}(\omega_{\mathrm{m}} - \omega_{\mathrm{L}}) \tag{6}$$

with

$$\frac{\mathrm{d}\theta_{\mathrm{m}}}{\mathrm{d}t} = \omega_{\mathrm{m}}, \quad \frac{\mathrm{d}\theta_{\mathrm{L}}}{\mathrm{d}t} = \omega_{\mathrm{L}} \tag{7}$$

where k_{s} (Nm/rad) is the spring constant, B_{m} and B_{L} (Nm/(rad/s)) are the viscous motor and load frictions, B_{s} (Nm/(rad/s)) is the inner damping coefficient of the shaft, J_{m} and J_{L} (kg m^2) are the motor and load moments of inertia, ω_{m} and ω_{L} (rad/s) are the motor and load angular speeds, T_{m} and T_{d} (Nm) are the motor and load disturbance torques and T_{s} (Nm) is the transmitted shaft torque.

2.1. Nonlinear model

Mechanical control systems are supposed to operate with high accuracy and speed despite adverse effects of system nonlinearities and uncertainties. This robustness property is of great importance if the system is part of a robotic or servo system, which requires insensitivity to unmodeled dynamics [12,14]. The linear model is capable of supplying the required robustness property when the mechanical system rotates in a single direction. In other words, as long as the rotational speed span of the system excludes the zero speed point, the linear model can be safely used in representing the system behavior for identification and control design purposes. The dominant nonlinear effects, like the dead zone and the Coulomb friction, can be approximated by linear dynamics for this case. However, if the system rotates in both directions, in other words, if the system output span includes the speed of zero, the dead zone and the Coulomb friction appear as hard nonlinearities that cannot be expressed in linear terms [1,8]. Consequently, the linear model lacks accuracy and reliability for this case.

Nonlinear friction models have been extensively discussed in the literature [8,10,14]. Nevertheless, there is considerable disagreement on the proper model structure. It is well established that the Coulomb friction torque is a function of the angular velocity. There is, however, disagreement concerning the character of the function. In the classical Coulomb friction model, there is a constant friction torque opposing the motion when $\omega = 0$ [10,15]. For zero velocity, the striction will oppose all motions as long as the torques are smaller in magnitude than the striction torque. The model has been well established in connection with slow speeds in numerically controlled machines [8]. In systems operating at relatively high speeds, the characteristic given in Fig. 3a is sufficient in representing the nonlinear Coulomb friction. For those systems, the Coulomb friction is expressed as a signum function dependent on the rotational speed [12]:
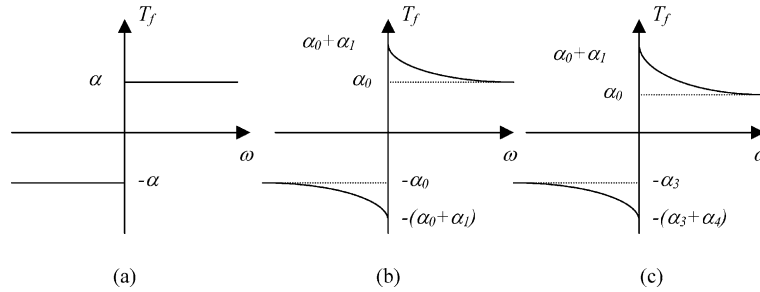
Fig. 3. Different nonlinear friction models.

$$T_f(\omega) = \alpha\,\mathrm{sgn}(\omega) \atop \forall\omega\in R \tag{8}$$

This characteristic is sufficient for representing rotational systems that operate at relatively high speeds but lacks accuracy when the operation is condensed around the zero speed. The mathematical models of the friction-velocity curve in Fig. 3b often represent the transition from static to kinetic friction by an exponential term in velocity. A more general model of this form, including Coulomb friction, is [8]:

$$T_f(\omega) = \alpha_0\,\mathrm{sgn}(\omega) + \alpha_1 e^{-\alpha_2|\omega|}\,\mathrm{sgn}(\omega) \atop \forall\omega\in R \tag{9}$$

where α_i are positive constants, $\alpha_i > 0$, $i = 0,1,2$ and $\alpha_i \in R$. The function sgn (the signum function) is defined as [15]:

$$\mathrm{sgn}(\omega) = \begin{cases} 1 & \omega > 0 \\ 0 & \omega = 0 \\ -1 & \omega < 0 \end{cases} \tag{10}$$

The model given in Eq. (9) includes the transition from static to kinetic friction represented by the exponential term and is more convenient for systems exhibiting very low speeds. It can easily be observed that the nonlinear friction representation in Eq. (8) is an approximation to the general representation in Eq. (9) for large values of $|\omega|$. A more generalized model for the nonlinear friction can be obtained by considering an asymmetrical characteristic as in Fig. 3c:

$$T_f(\omega) = \left(\alpha_0 + \alpha_1 e^{-\alpha_2|\omega|}\right)\mathrm{sgn}\,1(\omega) + \left(\alpha_3 + \alpha_4 e^{-\alpha_5|\omega|}\right)\mathrm{sgn}\,2(\omega) \atop \forall\omega\in R \tag{11}$$

where the functions sgn 1 and sgn 2 are defined as:

$$\mathrm{sgn}\,1(\omega) = \begin{cases} 1 & \omega \geqslant 0 \\ 0 & \omega < 0 \end{cases}, \quad \mathrm{sgn}\,2(\omega) = \begin{cases} 0 & \omega \geqslant 0 \\ -1 & \omega < 0 \end{cases}$$

$\alpha_i \in R$, $\alpha_i > 0$, $i = 0,\ldots,5$ and $\alpha_0 \neq \alpha_3$, $\alpha_1 \neq \alpha_4$, $\alpha_2 \neq \alpha_5$ in general. Obviously, the models in Eqs. (8) and (9) are special cases of the general model in Eq. (11). At low speed operations and servo applications, the model in Eq. (8) is insufficient in giving a thorough representation of the system behavior.
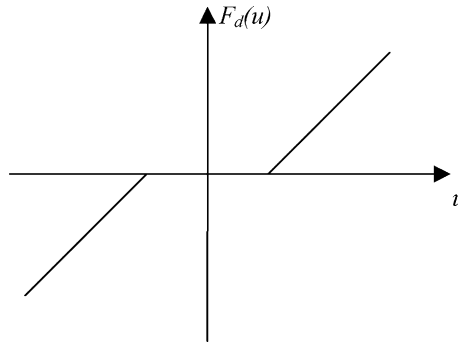
Fig. 4. Dead zone nonlinearity.

Dead zone nonlinearity is also a common type of nonlinear characteristic that occurs in many practical applications [16–19]. The ideal dead zone nonlinearity is given in Fig. 4 [15]. Such characteristic is typical of valves and some amplifiers at low input signals and occurs in many mechanical systems [16–19]. For the present case, the rotational system exhibits this type of nonlinearity when the armature voltage is around zero. When a continuous signal applied to the armature of the driving DC motor goes through zero volts, the system stays motionless for some time. This is a result of the fact that the mechanical system cannot respond immediately to input signal commands when it is at rest. The Coulomb friction causes mechanisms to be resistant to move from rest. A well known phenomenon concerned with Coulomb friction is that the rotational system will not start to move apparently until the driving torque is large enough to break the static friction torque. Such characteristics of Coulomb friction form a dead zone nonlinearity in the present system [10].

With the introduction of the nonlinear Coulomb friction and dead zone friction, the system model should be improved to represent the nonlinear system characteristics. The governing equations of system dynamics given in Eqs. (4) and (5) are modified to include the speed dependent friction as follows:

$$J_m \left(\frac{d\omega_m}{dt} \right) = T_m - T_s - B_m \omega_m - T_f(\omega_m) \tag{12}$$

$$J_L \left(\frac{d\omega_L}{dt} \right) = T_s - B_L \omega_L - T_d - T_f(\omega_L) \tag{13}$$

The block diagram for the nonlinear overall system is illustrated in Fig. 5. The Coulomb friction blocks represent the major nonlinearity in the system. In addition, as a result of the holding effects of static and Coulomb frictions, a dead zone nonlinearity is also introduced in the system. This nonlinearity cannot be located at a specific stage of the plant as a separate nonlinear block. Actually, the dead zone nonlinearity appears as a characteristic between the overall system input, which is the applied voltage of the DC motor, and the overall system output, which is the angular velocity of the load [10].
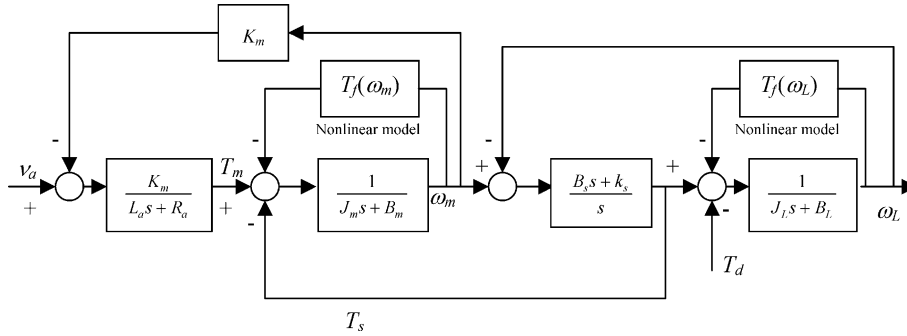
Fig. 5. Block diagram representing the nonlinear system.

3. Nonlinear system identification

The identification process consists of estimating the unknown parameters of the system dynamics [5]. Consequently, determination of the assumed system structure is of great importance in the process of system identification [6]. The linear model for the system results in a linear transfer function of order four, but this high order is a result of the fact that the two masses in the system, namely the motor and the load, have been considered separately. However, the total inertia in the system can be reflected to the motor shaft and the system model can be reduced to a single rotating element with one united moment of inertia [8], which makes the linear system model third order. This assumption is practically acceptable as far as the linear model is concerned [3,8,11], however, uniting the two inertias in the system leads to loss of the nonlinear friction torques in the system, which are the unmodeled dynamics of the system for the linear model. Choosing a higher order model gives little gain in accuracy for the linear model, but it may help in recovering the system nonlinearities that are not considered in the model [9].

The recursive least squares (RLS) method has been recommended for the identification process for easy implementation and application to real systems [5,6,20]. For the linear identification process, a discrete time ARX model for the mechatronic system has been used. This model structure is, in some sense, a linear regression form and permits easy implementation of the linear regression based identification [5]. The ARX model for the linear system is given as [6]:

$$A(q^{-1})y(t) = B(q^{-1})u(t) + e(t) \tag{14}$$

where

$$A(q^{-1}) = 1 + a_1 q^{-1} + a_2 q^{-2} + \cdots + a_{n_a} q^{-n_a},$$

$$B(q^{-1}) = b_0 + b_1 q^{-1} + b_2 q^{-2} + \cdots + b_{n_b} q^{-n_b}$$

and the symbol q^{-1} denotes the backward shift operator, $(y(t-1) = q^{-1}y(t))$, $u(t)$ and $y(t)$ are the system input and output, respectively, $e(t)$ is assumed to be an immeasurable, statistically independent noise sequence with $E\{e(t)\} = 0$ of variance σ_e^2. The parameters a_i and b_i are the real coefficients, $a_i, b_i \in R$, and n_a and n_b are the orders of the polynomials $A(q^{-1})$ and $B(q^{-1})$,
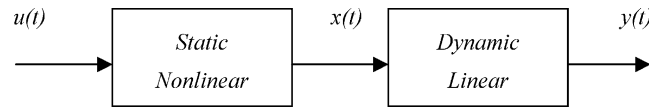
Fig. 6. Hammerstein system structure.

respectively, where $n_a \geqslant n_b$. It is also assumed that the polynomial $1 + \sum_{i=1}^{N} a_i q^{-i}$ never becomes zero in $|z| \geqslant 1$, and the model parameters a_i and b_i do not become zero simultaneously.

Identification of nonlinear systems can be achieved in a number of ways. Several methods for nonlinear system representation and identification have been proposed [5,6,20]. Nonparametric methods of nonlinear system identification do not require parametric expressions for the system nonlinearities. In addition, these methods have the advantage of applicability to nonlinear systems with dynamic nonlinearities [21,22]. However, these methods take the system as a whole and do not permit separate analysis and identification of the linear dynamics. With the assumption that the nonlinearities in the system are static, in other words, the system dynamics can be expressed in linear terms only, the parametric identification methods can be employed. This assumption leads to nonlinear system structures called the Hammerstein model, the Wiener model and the general NARMAX (Nonlinear Autoregressive Moving Average with Exogenous input) model [7]. The nonlinear Hammerstein model structure, given in Fig. 6, has several advantages, such as the nonlinear system identification problem can be put into linear regression form, methods of linear system identification can be applied and it can describe a nonlinearity of a dynamical system efficiently [21]. In addition, this structure covers a wide range of nonlinear systems despite its simplicity [7].

The dynamical linear part in the Hammerstein model can be represented by an ARX model as for the linear system model [7]. The relationship between the linear part input $x(t)$ and output $y(t)$ can be given as:

$$\tilde{A}(q^{-1})y(t) = \tilde{B}(q^{-1})x(t) + e(t) \tag{15}$$

where $x(t)$ is the output of the nonlinearity.

The nonlinear part in the Hammerstein model is generally chosen to be a polynomial of known order. The order of the polynomial is selected in accordance with the hardness of the nonlinearity in the system. The nonlinearity function $x(t)$ is given by [7]:

$$x(t) = \gamma_1 u(t) + \gamma_2 u^2(t) + \cdots + \gamma_n u^n(t) \tag{16}$$

where γ_j $(j = 1, \ldots, n,)$ are the nonlinearity parameters, $\gamma_j \in R$. The nonlinear equation, Eq. (16), is re-arranged to be [7]:

$$\tilde{A}(q^{-1})y(t) = \tilde{B}(q^{-1}) \sum_{j=1}^{n} \gamma_j u^j(t) + e(t) \tag{17}$$

In Eq. (17), the coefficients of $\tilde{B}(q^{-1})$ do not appear explicitly. Without loss of generality, the nonlinear part can be normalized with respect to γ_1, and Eq. (17) can be rewritten with the assumption that $\gamma_1 = 1$ as follows:

$$\tilde{A}(q^{-1})y(t) = \tilde{B}(q^{-1})u(t) + \sum_{j=2}^{n} \sum_{k=0}^{n_b} \tilde{b}_k \gamma_j q^{-k} u^j(t) + e(t) \tag{18}$$

Define a polynomial $S_j(q^{-1})$

$$S_j(q^{-1}) = \gamma_j \tilde{B}(q^{-1}) = s_{j0} + s_{j1} q^{-1} + \cdots + s_{jn_b} q^{-n_b} \tag{19}$$

where $s_{jk} = \gamma_j \tilde{b}_k$, $j = 1, \ldots, n$, $k = 0, \ldots, n_b$. Then, Eq. (18) is improved to be

$$\tilde{A}(q^{-1})y(t) = \tilde{B}(q^{-1})u(t) + \sum_{j=2}^{n} S_j(q^{-1}) u^j(t) + e(t) \tag{20}$$

Eq. (20) can be put into linear regression form as follows:

$$y(t) = \phi^T(t)\theta + e(t) \tag{21}$$

where

$$\phi(t) = \big(-y(t-1), -y(t-2), \ldots, -y(t-n_a), u(t), u(t-1), \ldots, u(t-n_b),$$
$$u^2(t), \ldots, u^2(t-n_b), \ldots, u^n(t), \ldots, u^n(t-n_b) \big)^T \tag{22}$$

$$\theta = \big(\tilde{a}_1, \tilde{a}_2, \ldots, \tilde{a}_{n_a}, \tilde{b}_0, \tilde{b}_1, \ldots, \tilde{b}_{n_b}, s_{20}, \ldots, s_{2n_b}, \ldots, s_{n0}, \ldots, s_{nn_b} \big) \tag{23}$$

The linear regression representation for the system given in Eq. (21) permits direct application of the RLS method. However, the vector of unknown parameters does not include the coefficients of the polynomial $\tilde{B}(q^{-1})$ explicitly. These coefficients are implicitly expressed in the form of products with the nonlinear subsystem parameters $\gamma_j (j = 1, \ldots, n)$. Consequently, the identification of the system parameters cannot be performed at a single stage. The RLS method is, therefore, implemented in two steps. The first step of the algorithm gives the estimates of the parameters a_i and s_{jk}, and the second step estimates the parameters b_k and γ_j using the results of the first step, where $i = 1, \ldots, n_a$, $j = 1, \ldots, n$, $k = 0, \ldots, n_b$. The nonlinear identification algorithm steps are summarized as follows:

 (i) Choose initial values for the covariance matrix P and forgetting factor λ.
 (ii) Acquire the input and output of the system and form the data vector ϕ as given in Eq. (22) for time instant t using the present and past values of the input u, output y and powers of u.
(iii) Solve for the parameter estimates $\hat{a}_i, \hat{b}_k, \hat{s}_{jk}$ using the RLS estimation rule:

$$\varepsilon(t) = y(t) - \phi^T(t)\hat{\theta}(t-1)$$
$$P(t) = \frac{1}{\lambda} P(t-1) \left[I_p - \frac{\phi(t)\phi^T(t)P(t-1)}{\lambda + \phi^T(t)P(t-1)\phi(t)} \right]$$
$$\hat{\theta}(t) = \hat{\theta}(t-1) + P(t)\phi(t)\varepsilon(t)$$

(iv) Solve for the estimates $\hat{\gamma}_j \; j = 1, \ldots, n$ using the estimated values $\hat{b}_k, \hat{s}_{jk}$ by the formula:

$$\hat{\gamma}_j = \left(\sum_{k=1}^{n_b} \hat{b}_k^2 \right)^{-1} \sum_{k=1}^{n_b} \hat{b}_k \hat{s}_{jk} \quad j = 2, \ldots, n.$$

(v) Update the time instant, $t = t + 1$. Return to step (ii).

The major nonlinearities in the mechatronic system of concern are the Coulomb frictions, which are expressed as nonlinear functions of the rotational speeds, and the dead zone nonlinearity, which occurs between the overall system input and output. Although the Coulomb frictions are modeled as static nonlinear functions in our system, they introduce dynamic nonlinearities in the system input–output characteristics. This is a natural consequence of the fact that the static nonlinearities appear at the feedback loops of the two rotating masses. However, the dead zone nonlinearity has no dynamic component and can be put into the static nonlinearity block in the Hammerstein model. Although the Coulomb frictions appear as dynamic nonlinearities in the overall system model, they will be assumed to have static characteristics and included in the static nonlinear block. The validity of this assumption will be discussed in accordance with the experimental results and observations.

4. Experimental setup

A diagram of the experimental setup is given in Fig. 7. Two signal generators are used to provide the test signal to the motor. The generators produce sinusoids of different amplitudes and frequencies, which are summed to constitute a persistently exciting signal for the identification process. The signals are carefully adjusted to provide very low speed operation, which is essential for examination of the system nonlinearities. The measured input–output data are transferred to the computer (Pentium III 700 MHz in speed with a memory of 256 MB RAM) by a data acquisition card (ADVANTECH PCL-1800, 330 kHz in speed, 12 bit high speed A/D converter
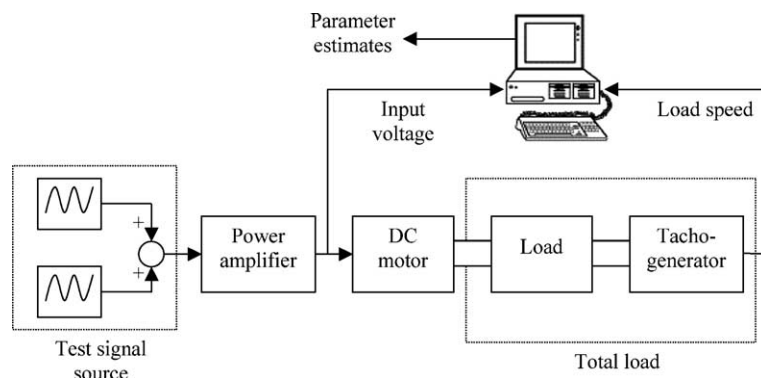

Fig. 7. Experimental setup for online nonlinear system identification.

with a conversion time of 2.5 μs). The data acquisition card permits use of user defined programs interfaced with Matlab.

The output speed is obtained from the tacho-generator. The output shaft speed is also measured from an optical sensor as rev/s that is connected to the motor shaft. The slotted opto sensor consists of a gallium–arsenide infrared LED and silicon phototransistor mounted in a special plastic case, which is transparent to light of the wavelength. A series of pulses is generated when the slotted disk that is mounted on the motor shaft is rotated. The permanent magnet DC motor to be studied operates at ±12 V input armature voltage with a maximum output shaft speed of 2400 rev/min. The motor drives a shaft that carries disks that operate various transducers and a tacho-generator.
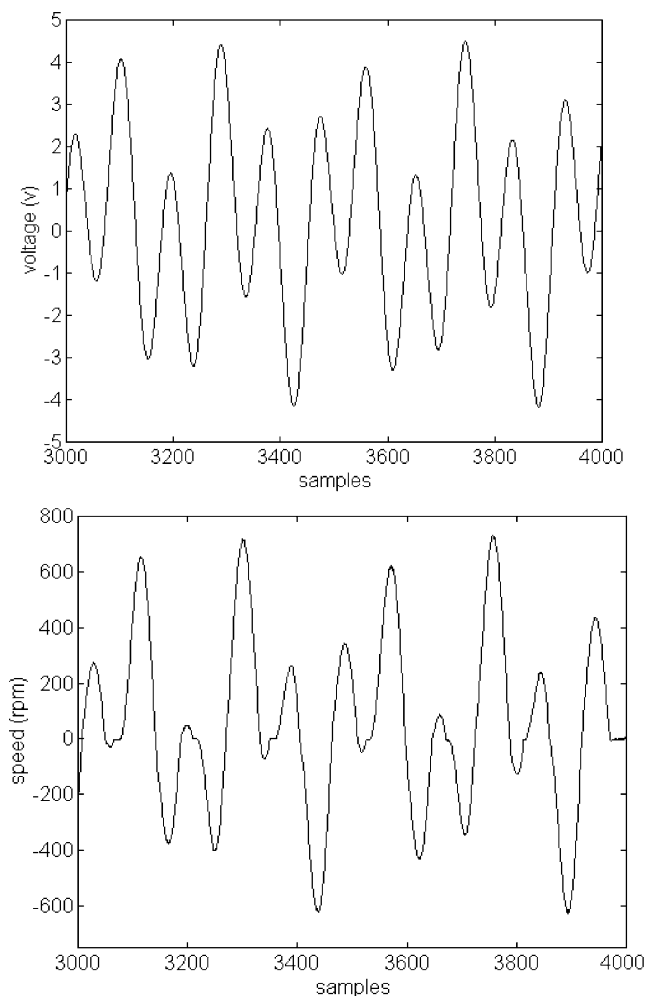

Fig. 8. Input signal (upper) and the system response (lower).

5. Experimental results

From the pretest experiments, the settling time of the system was measured to be about 400 ms. The sampling interval of the data acquisition process is chosen to be 40 ms, which is 10% of the step response settling time, for adequate recognition of the system dynamics and rejection of high frequency noise without pre-filtering [6]. The applied test signal varies around zero volts, which has been preferred for examination of the dead zone and Coulomb friction effects on the identified system. Time intervals where small amplitude variations around zero occur were intentionally
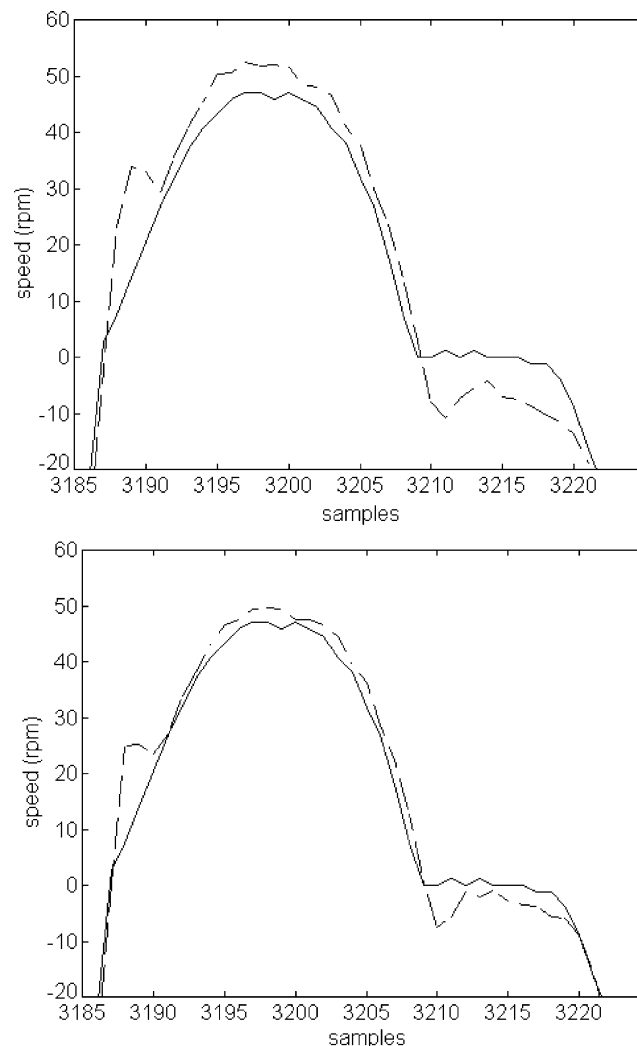

Fig. 9. Real system response (solid) and identified model response (dashed) for very low speeds with linear identification (upper) and nonlinear identification (lower).
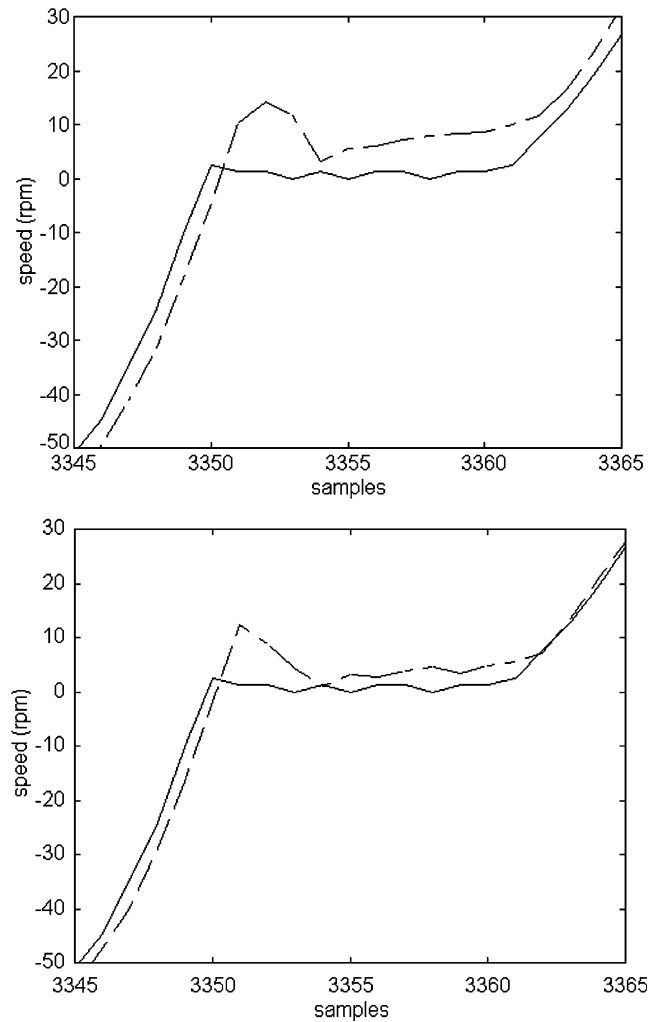
Fig. 10. Real system response (solid) and identified model response (dashed) for very low speeds with linear identification (upper) and nonlinear identification (lower).

produced for detection of the system nonlinearities at the system output. The test signal (armature voltage) and the response of the system are given in Fig. 8.

The results of the experiments performed using the setup given in Section 2 are illustrated by the graphs in Figs. 9–15. The plots in Figs. 9–11 give the output signals for the linear identification experiment and the nonlinear identification experiment. In all the figures, the solid lines give the measured real system output, and the dashed lines give the identified system output. The error between the actual output and the predicted output is smaller in the nonlinear identification compared with the linear identification.
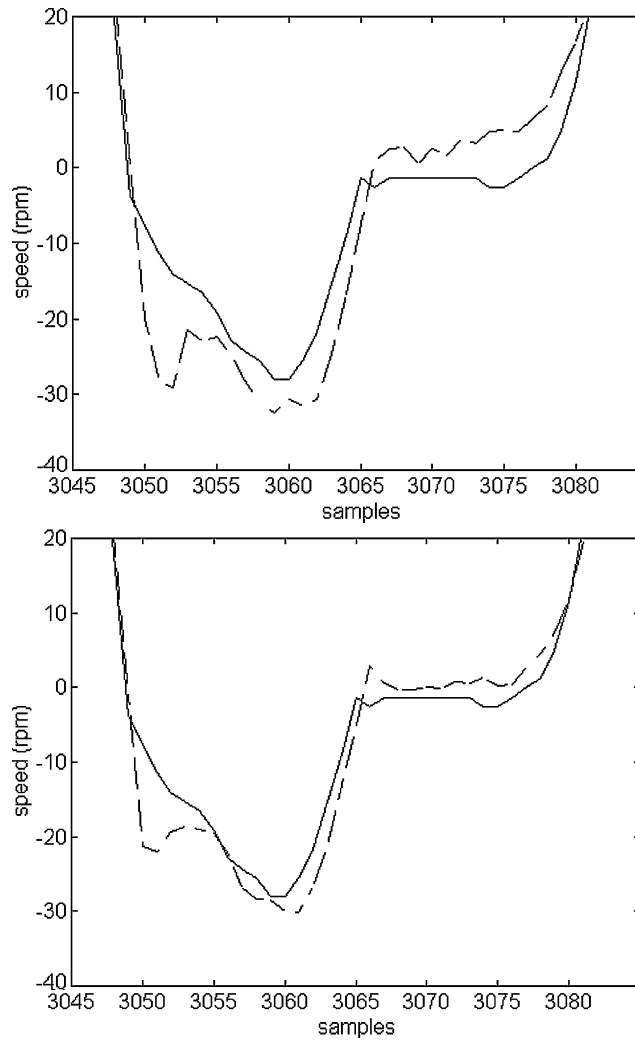
Fig. 11. Real system response (solid) and identified model response (dashed) for very low speeds with linear identification (upper) and nonlinear identification (lower).

5.1. Model validation

The mean square error (MSE) method is the most commonly used one for model testing purposes [23–25]:

$$\text{MSE} = \frac{1}{N} \sum_{t=1}^{N} (y(t) - \hat{y}(t))^2$$

where $\hat{y}(t)$ is the predicted output and N is the number of samples used in the identification process. The MSE values for the linear and nonlinear identification experiments were calculated for different model orders, and the results are tabulated in Table 1.
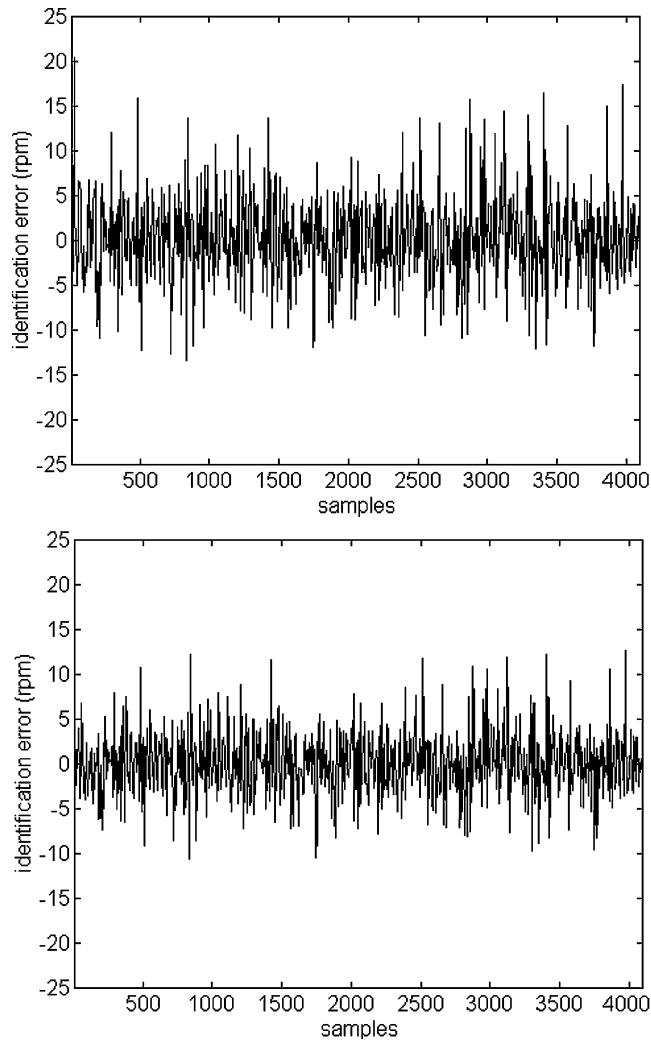
Fig. 12. Identification error for the linear model (upper) and the nonlinear model (lower).

During the nonlinear experiments, the order of the nonlinear polynomial was kept constant at three. The linear identification experiments result in the selection of the third or fourth order model for representing the present mechanical system. The difference between the MSE values for orders three and four is about 0.42%, so either of the two can be preferred without much loss in accuracy. The nonlinear identification results, however, reveal definitely that the fourth order model gives the best result as far as the identification error is concerned. Furthermore, the identification results indicate that the nonlinear system identification with fourth order linear dynamics gives the best result among all linear and nonlinear experiments.

The order of the nonlinearity, which is kept constant at three during the MSE tests, is also examined with a number of experiments. The MSE values for different orders of the nonlinear
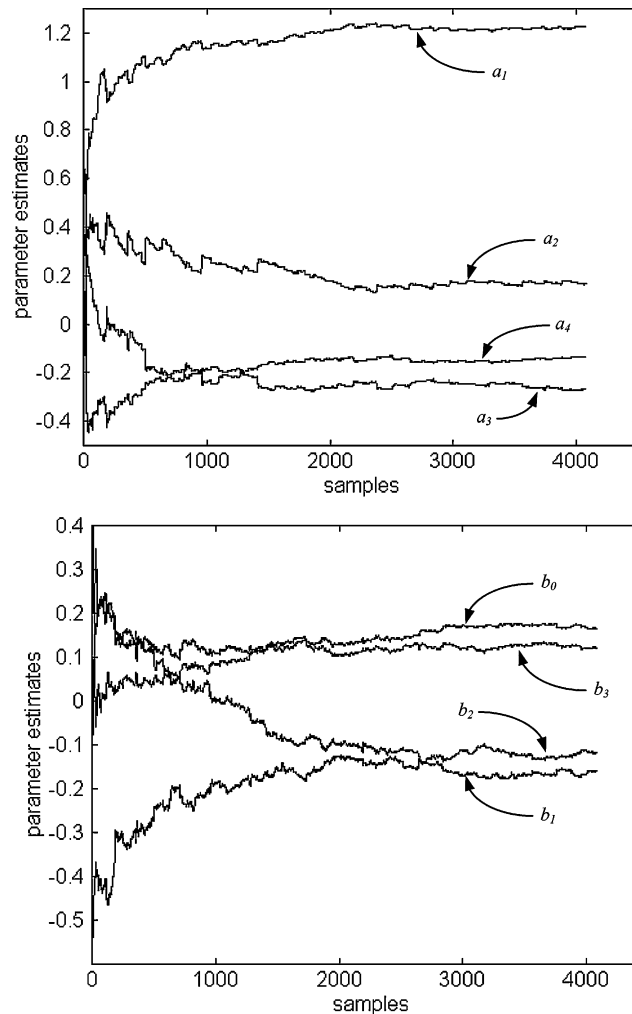
Fig. 13. Parameter estimates for the linear model: Coefficients of $A(q^{-1})$ (upper) and coefficients of $B(q^{-1})$ (lower).

polynomial were calculated and tabulated with the linear part of order four. The results presented in Table 2 reveal clearly that the selection of the third order nonlinearity in the nonlinear identification experiments gives the best result.

The results obtained clearly show that the identification accuracy is definitely improved in the nonlinear identification experiment, but the point to be emphasized here is where the improvement is condensed. In other words, the improvement in the identification performance is expected to focus where the nonlinearity occurs, which is around the zero speed. To have a better understanding of the performance of the nonlinear system identification method, a closer look at the low speed behavior of the motor is necessary.

The plots in Figs. 9–11 illustrate the low speed performances of the linear and nonlinear system identification experiments. Despite the relatively small improvement in the total identification
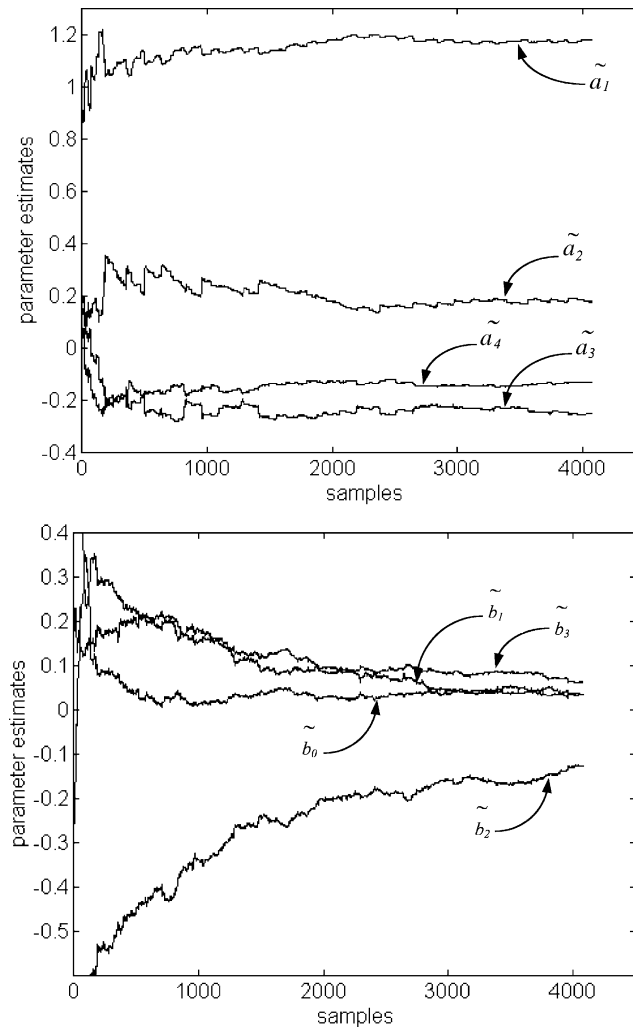
Fig. 14. Parameter estimates for the nonlinear model: Coefficients of $\tilde{A}(q^{-1})$ (upper) and coefficients of $\tilde{B}(q^{-1})$ (lower).

performance, the graphical results suggest that the ability of the identified system output to follow the real system behavior at low speeds considerably improves in the nonlinear identification case. The variation of the identification error, which is defined as the difference $y(t) - \hat{y}(t)$, is presented in Fig. 12 for the linear and nonlinear identification experiments. Fig. 12 clearly indicates the good output tracking performance of the nonlinear identification process with respect to the linear approach. The identified system output approaches the real system output in a shorter time with less fluctuation for the nonlinear case. This result is supported by the plots given in Figs. 13–15 as well. The variation of parameters identified using the linear and nonlinear approaches clearly indicate that the time needed for the estimates to converge is larger for the linear case.
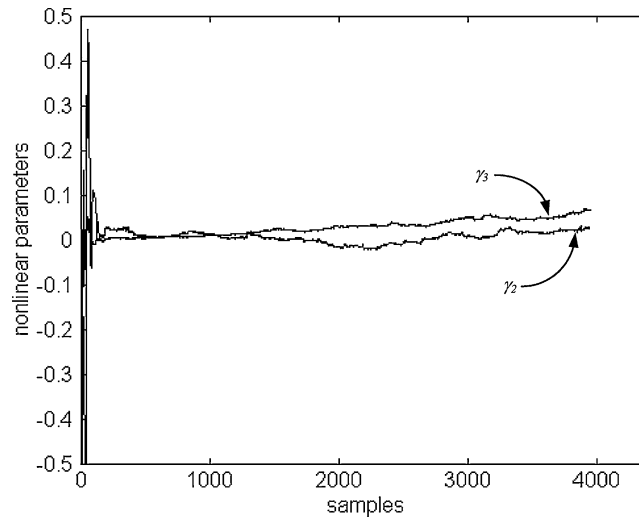
Fig. 15. Parameter estimates for the nonlinear model: Nonlinearity coefficients.

Table 1
MSE values for linear and nonlinear identification experiments

Model order	1	2	3	4	5	6
MSE, linear (rpm)	55.3203	29.1033	21.6595	21.4769	22.2718	22.1547
MSE, nonlinear (rpm)	47.3696	28.7214	20.0978	19.6518	21.1327	22.1244

Table 2
MSE values and nonlinear parameters for nonlinear identification with different polynomial orders

	Polynomial order (n)			
	2	3	4	5
MSE (rpm)	21.8216	19.6518	21.0330	34.5662
γ_2 ($\times 10^{-3}$)	0.43075	20.686	−0.030586	0.030137
γ_3 ($\times 10^{-3}$)	–	82.895	14.465	−0.23844
γ_4 ($\times 10^{-4}$)	–	–	−7.6866	−0.010632
γ_5 ($\times 10^{-6}$)	–	–	–	6.9051

6. Conclusion

The theoretical and experimental study on nonlinear modeling and identification of a two mass mechanical system with a DC motor rotating in two directions is presented in the present paper. Linear and nonlinear models were developed for the system. The nonlinear Coulomb friction and dead zone effects were taken into account, and a nonlinear representation and identification approach using the nonlinear Hammerstein system structure was used for the present system. A suitable experimental setup was built and tested using the RLS identification algorithm for the linear and nonlinear cases. The results are numerically and graphically demonstrated. These

revealed that the performance of the nonlinear approach was superior to that of the linear approach for low speed operation, where the nonlinearities in the system are effective. The identification error and the convergence properties of the estimates also seemed to improve with introduction of the nonlinear approach. The results of the present study are meant to constitute a starting point for ongoing studies on identification of mechanical systems by other nonlinear methods and adaptive control applications for nonlinear systems.

References

[1] Lyshevski SE. Nonlinear control of mechatronic systems with permanent-magnet DC motors. Mechatronics 1999;9:539–52.

[2] Yavin Y, Kemp PD. Modeling and control of the motion of a rolling disk: Effect of the motor dynamics on the dynamical model. Comput Meth Appl Mech Eng 2000;188:613–24.

[3] Horng JH. Neural adaptive tracking control of a DC motor. Informat Sci 1999;118:1–13.

[4] Mummadi VC. Steady-state and dynamic performance analysis of PV supplied DC motors fed from intermediate power converter. Solar Energy Mater Solar Cells 2000;61:365–81.

[5] Ljung L. System identification: Theory for the user. Englewood Cliffs, NJ, USA: Prentice Hall; 1987.

[6] Söderström T, Stoica P. System identification. Cambridge, UK: Prentice Hall; 1989.

[7] Kara T, Eker İ. Identification of Nonlinear Systems for Feedback Control. In: Proceedings of the Fourth GAP Engineering Congress 2002. p. 520–6.

[8] Jang JO, Jeon GJ. A parallel neuro-controller for DC motors containing nonlinear friction. Neurocomputing 2000;30:233–48.

[9] Nordin M, Gutman P. Controlling mechanical systems with backlash—A survey. Automatica 2002;38(10):1633–49.

[10] Wu R-H, Tung P-C. Studies of stick-slip friction, presliding displacement, and hunting. J Dyn Syst—Trans ASME 2002;124:111–7.

[11] Ogata K. Modern control engineering. USA: Prentice Hall Inc.; 1990.

[12] Slotine E, Li W. Applied nonlinear control. USA: Prentice Hall Inc.; 1991.

[13] Lee PL. Nonlinear process control: Applications of generic model control. GB: Springer-Verlag Ltd.; 1993.

[14] Lischinsky P, Canudas-de-Wit C, Morel G. Friction compensation for an industrial hydraulic robot. IEEE Contr Syst Mag 1999;19(1):25–32.

[15] Khalil HK. Nonlinear systems. NJ, USA: Prentice Hall; 2002.

[16] Liu GP, Daley S. Optimal-tuning nonlinear PID control of hydraulic systems. Control Eng Pract 2000;8(9):1045–53.

[17] Sun Y-J, Hsien Y-C, Hsieh J-G. A unifying control scheme of linear circuits with saturating or dead-zone actuator. J Franklin I 1997;334(3):427–30.

[18] Wang J, Pu J, Moore P. A practical control strategy for servo-pneumatic actuator systems. Control Eng Pract 1999;7(12):1483–8.

[19] Zongli L. Robust semi-global stabilization of linear systems with imperfect actuators. Syst Control Lett 1997;29(4):215–21.

[20] Hsia TC. System Identification. D.C. Heath and Co., USA, 1977.

[21] Sun L, Liu W, Sano A. Identification of a dynamical system with input nonlinearity. IEE Proc Control Theory Appl 1999;146(1):41–51.

[22] Hasiewicz Z. Hammerstein system identification by the Haar multiresolution approximation. Int J Adapt Control 1999;13:691–717.

[23] Chen YY, Jackson DA. An empirical study on estimators for linear regression analyses in fisheries and ecology. Fish Res 2000;49(2):193–206.

[24] Faber MN. Estimating the uncertainty in estimates of root mean square error of prediction: Application to determining the size of an adequate test set in multivariate calibration. Chemometr Intel Lab 1999;49(1):79–89.

[25] Wan ATK, Ohtani K. Minimum mean-squared error estimation in linear regression with an inequality constraint. J Stat Plan Infer 2000;86(1):157–73.